30 Jun 2012

Experimental and Computational Validation and Verification of the Stokes-Darcy and Continuum Pipe Flow Models for Karst Aquifers with Dual Porosity Structure

Xiaolong Hu

Xiaoming Wang
Missouri University of Science and Technology, xiaomingwang@mst.edu

Max Gunzburger

Fei Hua

et. al. For a complete list of authors, see https://scholarsmine.mst.edu/math_stat_facwork/1217

Recommended Citation

X. Hu et al., "Experimental and Computational Validation and Verification of the Stokes-Darcy and Continuum Pipe Flow Models for Karst Aquifers with Dual Porosity Structure," *Hydrological Processes*, vol. 26, no. 13, pp. 2031 - 2040, Wiley, Jun 2012.
The definitive version is available at https://doi.org/10.1002/hyp.8308

HYDROLOGICAL PROCESSES
Hydrol. Process. **26**, 2031–2040 (2012)
Published online 15 November 2011 in Wiley Online Library
(wileyonlinelibrary.com) DOI: 10.1002/hyp.8308

Experimental and computational validation and verification of the Stokes–Darcy and continuum pipe flow models for karst aquifers with dual porosity structure

Xiaolong Hu,[1,2]* Xiaoming Wang,[3] Max Gunzburger,[4] Fei Hua[3,4] and Yanzhao Cao[5]

[1] *School of Water Resources and Environmental Sciences, China University of Geosciences, Beijing 100083, China*
[2] *Department of Earth, Ocean and Atmospheric Sciences, Florida State University, Tallahassee, FL, 32306, USA*
[3] *Department of Mathematics, Florida State University, Tallahassee, FL, 323064, USA*
[4] *Department of Computation Sciences, Florida State University, Tallahassee, FL, 32306, USA*
[5] *Department of Mathematics and Statistics, Auburn University, Auburn, AL, 36830, USA*

Abstract:

In our previous study, we developed the Stokes–Darcy (SD) model was developed for flow in a karst aquifer with a conduit bedded in matrix, and the Beavers–Joseph (BJ) condition was used to describe the matrix–conduit interface. We also studied the mathematical well-posedness of a coupled continuum pipe flow (CCPF) model as well as convergence rates of its finite element approximation. In this study, to compare the SD model with the CCPF model, we used numerical analyses to validate finite element discretisation methods for the two models. Using computational experiments, simulation codes implementing the finite element discretisations are then verified. Further model validation studies are based on the results of laboratory experiments. Comparing the results of computer simulations and experiments, we concluded that the SD model with the Beavers–Joseph interface condition is a valid model for conduit–matrix systems. On the other hand, the CCPF model with the value of the exchange parameter chosen within the range suggested in the literature perhaps does not result in good agreement with experimental observations. We then examined the sensitivity of the CCPF model with respect to the exchange parameter, concluding that, as has previously been noted, the model is highly sensitive for small values of the exchange parameter. However, for larger values, the model becomes less sensitive and, more important, also produces results that are in better agreement with experimental observations. This suggests that the CCPF model may also produce accurate simulation results, if one chooses larger values of the exchange parameter than those suggested in the literature. Copyright © 2011 John Wiley & Sons, Ltd.

KEY WORDS karst aquifer; conduit and matrix domains; pipe flow model; Stokes equation; Beavers–Joseph boundary; mass exchange rate

Received 4 March 2011; Accepted 30 August 2011

INTRODUCTION

Karst aquifers are susceptible to greater contamination than non-karstic aquifers because of rapid transport processes and limited chemical filtering capacities, both of which quicken the spread of solutes (Taylor and Greene, 2001; Matusick and Zanbergen, 2007; Kuniansky, 2008). In comparison with the large amount of modelling studies on groundwater flow and contaminant migration in porous and fractured media, similar studies on karst aquifers are very limited and inaccurate, although, in many states, karst aquifers represent a very significant source of water for public and private use (Kincaid, 2004). A karst aquifer, in addition to a porous limestone matrix, typically has large cavernous conduits that are known to largely control groundwater flow and contaminant transport within the aquifer (Katz *et al*., 1998). During a high-flow event, the water pressure in the conduits is larger than that in the ambient matrix so that conduit-borne contaminants can be driven into the matrix. During a low-flow event, the pressure differential reverses and contaminants sequestered in the matrix can be released into the free flow in the conduits and exit through, for example, springs and wells, into surface water systems (Li *et al*., 2008). This retention and release phenomenon induces an environmental issue in that sequestered contaminants may influence the quality of groundwater sources for a long time and thus significantly decrease water availability. Figure 1 provides a sketch of the conceptual model of a karst aquifer (Faulkner *et al*., 2009). In Figure 1, Ω_m and Ω_c denote the matrix and the conduit domains, respectively; Γg indicates the ground surface; Γ_{si} and Γ_{sp} indicate a sinkhole and spring boundary, respectively; Γ_{cm} indicates the conduit–matrix interface boundary; and Γ_0 indicates a bounding surface that is presumably far removed from the region of interest.

The dual character of a karst flow system is widely recognised and stems from the existence of different porosities within a karst aquifer (Ford, 1998; Worthington, 2003), which determines the type of flow prevailing in the

*Correspondence to: Correspondence to: Xiaolong Hu, School of Water Resources and Environmental Sciences, China University of Geosciences, Beijing 100083, China. E-mail: bill.x.hu@gmail.com

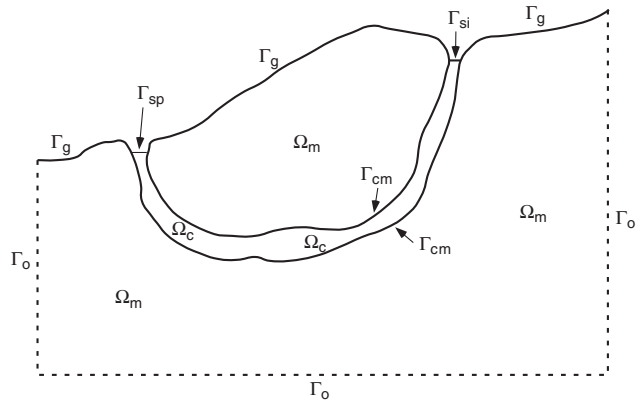

Figure 1. Conceptual model of a karst aquifer having a conduit Ω_c embedded in a matrixΩ_m

aquifer (Ford and Williams, 1989; Bauer *et al*., 2003). Similar to the dual-porosity/permeability model widely used for fractured media (Gerke and van Genuchten, 1993a, 1993b), the coupled continuum pipe flow (CCPF) model has been proposed to describe the flow and solute transport in karst aquifers (Chen and Bian, 1988; Kiraly, 1998; Bauer *et al*., 2000, 2003; Birk *et al*., 2003; MacQuarrie and Sudicky, 1996). The CCPF model is a dual flow system consisting of a matrix representing the bulk mass of permeable limestone and a conduit system representing the karst conduit network. Flow exchange between the two systems is controlled by differences in hydraulic heads as well as the hydraulic conductivity and the geometric setting. In the CCPF model, the groundwater flow in the matrix is described by the Darcy's law, and the flow in the conduit is modelled by a pipe flow model. The water mass exchange flow rate between the two systems, q_{ex}, is described by a first-order mass exchange model; the exchange flow rate is assumed to be linearly proportional to the head difference between the two systems (Barenblatt *et al*., 1960; Cao *et al*., 1988; Teutsch, 1989; Sauter, 1992; Cao *et al*., 2011). The exchange rate coefficient is a lumped parameter, and its value will depend on many factors including, among others, the hydraulic conductivity in the matrix, the exchange surface between the conduit and the matrix and the conduit geometry (Barenblatt *et al*., 1960; Liedl *et al*., 2003). The value of the exchange rate parameter is not usually obtained from measurements but rather through curve fitting. On the basis of the CCPF model, a new numerical method has been developed and became part of the new MODFLOW software (Shoemaker *et al*., 2008). Cao *et al*. (2011) studied the mathematical well-posedness of the CCPF model as well as convergence rates of finite element approximation established in the two-dimensional case. However, the suitability and validity of the CCPF as a model for groundwater flow in a karst aquifer, especially for the flow exchange between the matrix and the conduit, has not been well studied. In addition, the determination of the value of the exchange rate parameter is also an issue that needs attention.

Flow in karst aquifers, and especially the exchange of water and contaminants between the matrix and the conduit, can also be modelled by coupling the Darcy model for the flow in the matrix with the Navier–Stokes equations (or Stokes under low Reynolds number assumption) for the flow in the conduits. In this case, we have three-dimensional conduits (in contrast to the one-dimensional conduits of the pipe flow model) embedded in the matrix, and the exchange of water and water-borne contaminants occurs at the boundaries between the matrix and the conduit. In the study of Beavers and Joseph (1967), interface conditions, called the *Beavers–Joseph (BJ) conditions*, governing that exchange were developed on the basis of experimental observations; these have become widely accepted. However, the BJ conditions engender mathematical and computational difficulties so that several simplifications have been proposed (Saffman, 1971; Discacciati *et al*., 2002). Faulkner *et al*. (2009) developed the Stokes–Darcy (SD) method for flow in a karst aquifer with a conduit bedded in matrix. The BJ interface condition was used to describe the matrix–conduit interface.

The purpose of this study is to use mathematical, computational and experimental means for the verification and validation of the SD and CCPF models and of finite element discretisation algorithms and their implementations. Obtaining information about good choices for the values of the exchange parameters appearing in the models is also an objective of this study.

In the section on Models for Matrix–Conduit Flows, we provide descriptions of the SD and CCPF models and briefly touch on the mathematical issues of well-posedness of the models and on mathematical and computational results obtained from finite element discretisations. For the SD model, the results of asymptotic comparisons of the SD models with the BJ condition are provided, using the more sophisticated Stokes–Brinkman model as a benchmark. In the section on Experimental Validation of Simulation Models, we compare results obtained from the two models with results obtained from laboratory experiments. In the section on Sensitivities of Modeling Parameters, we use results obtained with the CCPF model to study the sensitivity of that model with respect to a modelling parameter (the exchange rate coefficient) and, using the validated SD model as a benchmark, glean some insight as to effective choices for the value of that parameter. Finally, in the section on Summary and Conclusions, we provide some concluding remarks.

MODELS FOR MATRIX–CONDUIT FLOWS

In this section, we considered two models for determining flow velocities and pressures in karst-like systems consisting of a porous matrix in which conduits are embedded. For both models, the Darcy equation is used for the flow in the matrix; for the free flow in the conduits, one uses a one-dimensional pipe flow model whereas the other uses the Stokes equations. A particularly important aspect we addressed was the proper accounting of the fluid exchange between the matrix and the conduit. The velocity field in the matrix, $\mathbf{V}_m$, determined from either the coupled pipe flow Darcy or the coupled SD systems is used in the governing equation for the conservative solute transport in the matrix

$$\frac{\partial C_{\mathrm{m}}}{\partial t} + \mathbf{V}_{\mathrm{m}}\cdot\nabla C_{\mathrm{m}} - \nabla\cdot(D_{\mathrm{m}}\nabla C_{\mathrm{m}}) = F_{\mathrm{m}} \qquad (1)$$

where C_{m} denotes the solute concentration in the matrix, D_{m} is the dispersion coefficient and F_{m} is the solute sources and sinks. Ideally, one should couple the tracer density in the matrix and conduit. However, assuming that the flow in the channel moves significantly faster than that in the matrix, we simply imposed a Dirichlet boundary condition for C_{m} along the matrix–conduit interface and a homogeneous Neumann boundary condition elsewhere on the matrix boundary.

SD model

SD model formulation. As shown in Figure 1, we denoted by Ω_{m} the domain occupied by the porous media and by Ω_{c} the one-dimensional (possibly) curved pipes that we used as surrogates for the embedded conduits. The conduits are modelled by one-dimensional curves, imbued with a diameter parameter d. We considered SD models for coupled conduit–matrix flows.

The flow in the porous matrix is modelled by a continuum approach using the Boussinesq equation (Bear and Verruijt, 1987),

$$S_{\mathrm{s}}\frac{\partial h_{\mathrm{m}}}{\partial t} + \nabla\cdot(-\mathbf{K}\nabla h_{\mathrm{m}}) = f_{\mathrm{m}} \quad \text{in} \quad \Omega_{\mathrm{m}} \qquad (2)$$

where $\boldsymbol{K}(x, y, z)$ denotes the hydraulic conductivity (L/T), S_{s} is the specific storage coefficient (L^{-1}) and f_{m} represents the sink/source term (T^{-1}). The hydraulic head h_{m} (L) is defined by $h_{\mathrm{m}} = z + \frac{p_{\mathrm{m}}}{\rho g}$, where p_{m}denotes the water pressure (M/LT^2), ρ is the water density (M/L^3), g is the gravitational constant (L/T^2) and z is the height (L).

We imposed the boundary conditions

$$\begin{aligned} &p_{\mathrm{m}} = 0 \text{ on } \Gamma_{\mathrm{sp}}, \Gamma_{\mathrm{si}} \text{ and groundwater table, } \mathrm{K}\nabla h_{\mathrm{m}}\cdot n \\ &\quad = 0 \text{ on } \Gamma_0 \end{aligned} \qquad (3)$$

where the first of which implies that the pressure on Γ_{sp}, Γ_{si} and groundwater table is zero and the second is a reasonable fictitious boundary condition useful for analysis and simulation purposes.

In the conduit domain,Ω_c, the other domain of the problem, the Navier–Stokes equations govern the free flow that is assumed to be incompressible (Faulkner *et al.*, 2009):

$$\left.\begin{aligned} \frac{\partial \mathbf{V}_{\mathrm{c}}}{\partial t} - \nabla\cdot\mathbf{T} &= f_{\mathrm{c}} \\ \nabla\cdot\mathbf{V}_{\mathrm{c}} &= 0 \\ \mathbf{V}_{\mathrm{c}}(\mathbf{x}, t=0) &= \mathbf{V}_0 \end{aligned}\right\} \quad \text{in} \quad \Omega_{\mathrm{c}} \qquad (4)$$

where $\mathbf{V}_{\mathrm{c}}$ denotes the fluid velocity, $\mathbf{T}(\mathbf{V}_{\mathrm{c}}, p) = -p_{\mathrm{c}}\mathbf{I} + 2\nu\mathbf{D}(\mathbf{V}_{\mathrm{c}})$ indicates the stress tensor, p_{c} is the kinetic fluid pressure (pressure divided by fluid density), $\mathbf{D}(V_{\mathrm{c}}) = \frac{1}{2}\left(\nabla V_{\mathrm{c}} + (\nabla V_{\mathrm{c}})^T\right)$ is the deformation tensor, $\boldsymbol{I}$ represents the identity matrix here in the definition of the stress tensor $\boldsymbol{T}$, ν is the kinetic viscosity of the fluid (viscosity divided by fluid density) and f_{c} is the general body forcing term.

At the sinkhole and the spring, we applied nonhomogeneous Dirichlet boundary conditions that specify the inflow and outflow velocities, respectively. Specifically, we set

$$\mathbf{V_c} \times n = 0 \text{ and } \mathbf{V_c}\cdot n = f_{\mathrm{si}} \text{ on } \Gamma_{\mathrm{si}} \qquad (5a)$$

$$\mathbf{V_c} \times \mathrm{n} = 0 \text{ and } \mathbf{V_c}\cdot \mathrm{n} = f_{\mathrm{sp}} \text{ on } \Gamma_{\mathrm{sp}} \qquad (5b)$$

where f_{si} and f_{sp} are inflow and outflow discharges at the spring and sinkhole, respectively, and the discharges are perpendicular to the water surface. The boundary conditions tell us that the discharges are perpendicular to the water surface. The discharge amounts, f_{si} and f_{sp}, in the sinkhole and spring, respectively, are determined from field measurements.

Along Γ_{cm}, the interface boundary between the matrix and the conduit, we applied the BJ conditions (Beavers and Joseph 1967),

$$\left.\begin{aligned} \mathbf{V}_c\cdot\mathbf{n}_{cm} &= \mathbf{V}_m\cdot\mathbf{n}_{cm} \\ -\mathbf{n}_{\mathrm{cm}}^T\cdot T(\mathbf{V}_{\mathrm{c}}, p)\cdot\mathbf{n}_{\mathrm{cm}} &= p = {}^{c}p_{\mathrm{m}} = g(h_{\mathrm{m}} - z) \\ -\tau_i^T\mathbf{D}(\mathbf{V}_{\mathrm{c}})\cdot\mathbf{n}_{\mathrm{cm}} &= \frac{\alpha_{\mathrm{sd}}\nu\sqrt{3}}{\sqrt{\mathrm{trace}(\boldsymbol{\Pi})}}\tau_i^T(\mathbf{V}_{\mathrm{c}} - \mathbf{V}_{\mathrm{m}}), i = 1, 2 \end{aligned}\right\} on\,\Gamma_{\mathrm{cm}} \qquad (6)$$

where $\{\tau_1, \tau_2\}$ represents a local orthonormal basis to the tangent plane to Γ_{cm}, $\boldsymbol{n}_{\mathrm{cm}}$ denotes the unit normal to Γ_{cm} pointing from the conduit to the matrix, g is the gravitational acceleration, α_{sd} is a constant parameter,$\boldsymbol{\Pi}$ is the intrinsic permeability that satisfies $\mathbf{K} = \boldsymbol{\Pi}g/\gamma$ and $\mathrm{trace}(\boldsymbol{\Pi}) = \sum_i \Pi_{ii} (i = 2\mathrm{or}3)$. The first condition states that the water mass flow is conserved across ${}_{?}\Gamma_{\mathrm{cm}}$, the second one is the balance of forces normal to the interface and the third interface condition relates the viscous drag forcing on the interface to the jump in tangential velocity. Justifications for the BJ interface conditions can be found in the work of Beavers and Joseph (1967).

Verification of finite element discretisations of the SD model. For the SD mathematical model developed in the section on SD model formulation, we applied a finite element method to numerically solve the model. For the computational experiments, we set $\Omega_{\mathrm{m}} = (0, 1) \times (0, 0.75)$ and $\Omega_{\mathrm{c}} = (0, 1) \times (-0.25, 0)$ so that the interface Γ_{cm} is given by $(0, 1) \times \{0\}$. For simplicity, all the parameters appearing in the SD model with the BJ boundary condition are set to unity, and the Dirichlet boundary conditions for $\mathbf{V}_{\mathrm{c}}$ and h_{m} are applied on the boundary. The finite element spaces are defined with respect to a uniform grid. The Taylor–Hood element pair, that is, continuous piecewise quadratic polynomials for the velocity components and continuous piecewise linear polynomials for the pressure, is used for the spatial discretisation of the Stokes system. The Darcy system is discretised using continuous piecewise quadratic polynomials. The backward Euler method with a constant time step is used to temporal discretisation. Error estimates are derived for this discretisation scheme; a typical result is that, for sufficiently smooth exact solutions (Hua, 2009),

$$\left\|v_c - v_c^{fe}\right\| + [\![h_m - h_m^{fe}]\!] \le C\left(h^3 + \Delta t\right) \tag{7}$$

for a constant C whose value does not depend on the spatial grid size h or the time step Δt; in Equation (7), $(\cdot)^{fe}$ denotes the finite element solution. Error estimates for a steady state case are obtained by omitting the term depending on Δt. Of course, a better rate of convergence with respect to Δt can be obtained if one uses a higher-order temporal discretisation scheme and the exact solution is sufficiently smooth. Using the method of manufactured solutions, we set the data in the differential equations, boundary conditions and initial condition so that the exact solution of the SD problem is given by (Hua, 2009)

$$\begin{bmatrix} u_c = [x^2y^2 + e^{-y}]\cos(2\pi t) \\ v_c = \left[-\frac{2}{3}xy^3 + [2 - \pi\sin(\pi x)]\right]\cos(2\pi t) \\ p_c = -[2 - \pi\sin(\pi x)]\cos(2\pi y)\cos(2\pi t) \\ h_m = [2 - \pi\sin(\pi x)][-y + \cos(\pi(1-y))]\cos(2\pi t) \end{bmatrix} \tag{8}$$

We first considered a steady-state case for which the exact solution is chosen by setting $t = 0$ in the previous expressions. Table I gives the computationally derived convergence rates as well as errors for this steady-state problem. We then considered the time-dependent problem; on the basis of the error estimate (Equation (7), we chose the time step to be related to the spatial grid size by $\Delta t \sim h^3$ so that, according to that estimate, spatial and temporal errors should be equilibrated. (A less onerous time step–spatial grid size relationship would be obtained if a higher-order temporal discretisation is used. For the purposes of this article, the discretisation methods we used suffice.)

The resulting errors and rates of convergence are given in Table II. The results in both tables indicate that the finite element approximations converge at the optimal rate for the discretisation schemes used; in particular, they are in agreement with the error estimate (Bobok, 1993).

Table I. Errors and convergence rates for the steady-state SD problem

h	$e_{u,0}$	$e_{u,1}$	$e_{p,0}$	$e_{h,0}$	$e_{h,1}$
2^{-3}	2.83E-04	1.08E-02	8.57E-03	5.48E-04	3.12E-02
2^{-4}	3.63E-05	2.67E-03	1.93E-03	5.99E-05	7.78E-03
2^{-5}	4.61E-06	6.64E-04	4.65E-04	7.085E-06	1.94E-03
2^{-6}	5.80E-07	1.66E-04	1.15E-04	8.68E-07	4.86E-04
rate	2.976	2.009	2.070	3.099	2.001

Column headings correspond to $e_{u,0} = \left\|u_c - u_c^{fe}\right\|_0$, $e_{u,1} = \left\|u_c - u_c^{fe}\right\|_1$, $e_{p,0} = \left\|p_c - p_c^{fe}\right\|_0$, $e_{h,0} = \left\|h_m - h_m^{fe}\right\|_0$ and $e_{h,1} = \left\|h_m - h_m^{fe}\right\|_1$.

Table II. Errors and convergence rates for the time dependent SD problem with $\Delta t \sim h^3$

h	$e_{u,0}$	$e_{u,1}$	$e_{p,0}$	$e_{h,0}$	$e_{h,1}$
2^{-3}	1.11E−03	1.47E−02	1.56E−02	3.68E−03	4.31E−02
2^{-4}	1.43E−04	3.01E−03	2.18E−03	4.61E−04	9.26E−03
2^{-5}	1.80E−05	6.92E−04	4.30E−04	5.73E−05	2.12E−03
2^{-6}	2.25E−06	1.68E−04	1.06E−04	7.12E−06	5.08E−04
Rate	2.984	2.143	2.394	3.005	2.135

Coupled continuum pipe flow model

CCPF model formulation. We denoted by Ω_m the domain occupied by the porous media and by Ω_p the one-dimensional (possibly) curved pipes that we used as surrogates for the embedded conduits. For the CCPF model, the conceptual model sketched in Figure 1 reduces to that in Figure 2.

Cao *et al*. (2011) developed a CCPF model,

$$S\frac{\partial h_m}{\partial t} - \nabla(K\nabla h_m) = -\alpha_{ccpf}(h_m - h_c)\delta_{\Omega_c} + f_m \text{ in } \Omega_m \tag{9a}$$

$$-\frac{\partial}{\partial\tau}\left(D\frac{\partial h_c}{\partial\tau}\right) = \alpha_{ccpf}(h_m - h_c) + f_c \text{ along } \Omega_c \tag{9b}$$

where h_m and h_c are the hydraulic heads in matrix and conduit, respectively; f_m and f_c are the sink/source terms in matrix and conduit, respectively; α_{ccpf} denotes the exchange rate coefficient between conduit and matrix; $\delta_{\Omega c}$ represents the Dirac δ function concentrated on Ω_c; $D = \frac{\pi d^4 g}{128\nu}$ is for three dimensions or $D = \frac{d^3 g}{12\nu}$ is for two dimensions, where d is the diameter of the tube, g is the gravitational acceleration, ν is the kinematic viscosity of water and Q is the total discharge in the pipe.

In this article, we considered a simplified, steady-state, two-dimensional setting. The following geometrical setup is used. The matrix continuum is assumed to occupy the square $\Omega_m = \{0 < x < 1,\ -½ < y < ½\}$ and the one-dimensional conduit pipe lies in the middle so that $\Omega_c = \{0 < x < 1;\ y = 0\}$. Then, Equation (9) reduces to

$$-\nabla(K\nabla h_m) = -\alpha_{ccpf}(h_m(x,0) - h_c(x))\delta(y) + f_m \text{ in } \Omega_m \tag{10a}$$

$$-\frac{\partial}{\partial\tau}\left(D\frac{\partial h_c}{\partial\tau}\right) = \alpha_{ccpf}((h_m|y=0) - h_c) + f_c \text{ in } \Omega_c \tag{10b}$$

where $\delta(y)$ denotes the Dirac delta function in y. In addition, we imposed the fixed-head (Dirichlet) boundary conditions for the purpose of numerical analysis

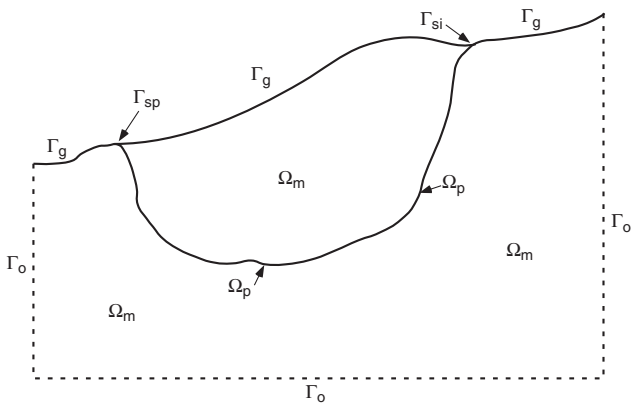

Figure 2. For the CCPF model, the conduit Ω_p in the conceptual model of a karst aquifer is a (one-dimensional) curve, and the sinkhole and spring boundaries Γ_{si} and Γ_{sp} are the end points of the curve, respectively

$$h_m = g_m \text{ on } \partial\Omega_m = \text{boundary of } \Omega_m \quad (11a)$$

$$h_c = g_{c0} \text{ at } x = 0;\ h_c = g_{c1} \text{ at } x = 1 \quad (11b)$$

where g_m is a given function and g_{c0} and g_{c1} are given numbers. In simulations, fixed flow rate (Neumann) boundary condition can be applied to the ends of the conduit as well.

In Cao *et al*. (2011), it is proved that, in the steady-state case, the two-dimensional problem (Equations (10) and (11)) is well posed, that is, a unique solution exists and, in appropriate norms, depends continuously on the data, that is, the forcing terms f_m and f_c. Additional regularity of the solution is also proved if the given data are smoother than that required for the existence of the solution. A finite element method for the discretisation of Equations (10) and (11) is developed and analysed. The well-posedness of the discrete problem obtained from the finite element discretisation is proved, and error estimates are derived for the cases of continuous piecewise linear and quadratic finite element functions.

In summary, we have used analytical and computational approaches to validate both the SD model with BJ boundary condition and CCPF model with first-order mass exchange between the two domains and to verify the correctness of the finite element codes developed to obtain approximate solutions for the models.

EXPERIMENTAL VALIDATION OF SIMULATION MODELS

In the section on Models for Matrix–Conduit Flows, we provide mathematical and computational verifications that the finite element simulation codes we developed for

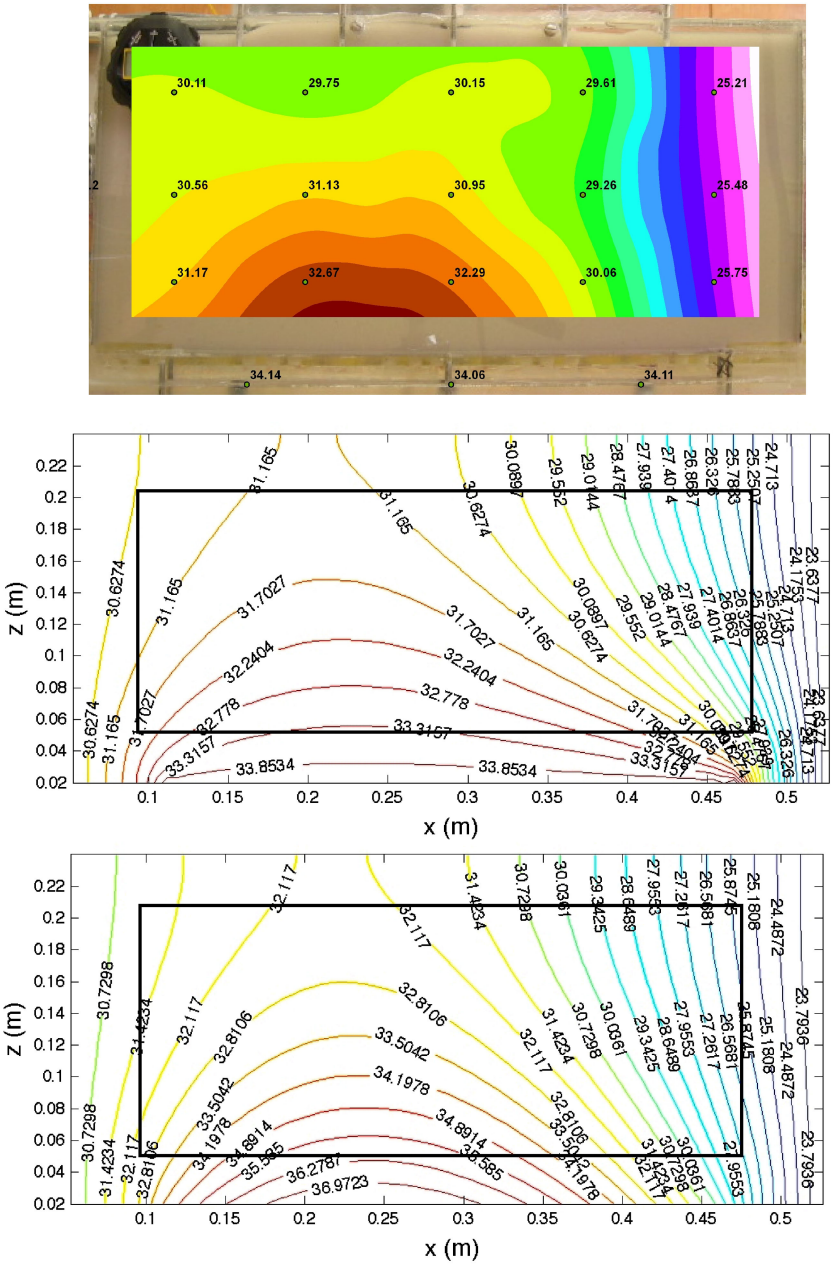

Figure 3. Experimental (top) and computational CCPF (middle) and SD (bottom) head distributions in the matrix

solving the SD and CCPF models produce accurate results. What remains is to validate either or both models through comparisons with experimental results. Furthermore, both models contain a tuning 'parameter', that is, α_{sd} in Equation (6) and α_{ccpf} in Equation (9). Thus, we used the experimental results of Faulkner *et al*. (2009) to obtain some guidance about the value of these parameters. The experimental facilities and procedure are described in Faulkner *et al*. (2009). Here, we just used the results to compare with the numerical simulations.

The model parameters used in the computer simulations are determined from the calibration of the experiment, for example, the matrix porosity and hydraulic conductivity, or from the literature. Bauer *et al*. (2003), Birk *et al*. (2003) and Liedl *et al*. (2003) concluded that the value of the exchange rate coefficient in the CCPF model α_{ccpf} should be proportional to the hydraulic conductivity $\boldsymbol{K}$ and also depend on the surface area available for the exchange of fluid between the matrix and the conduit. On the basis of these observations and calibrations of the matrix used in the experimental setup, a value of $\alpha_{ccpf} = 7 \times 10^{-4}\ \mathrm{m/s^2}$ was chosen for simulations.

For the parameter appearing in the BJ interface condition, we used the value $\alpha_{sd} = 0.2$, which is in the range suggested by Beavers and Joseph (1967). Figure 3 shows the hydraulic head distribution obtained from the experiments and from computer simulations on the basis of the SD and CCPF models. One observes that the SD simulation results are very close to the experimental results, whereas the CCPF model generally overestimates the hydraulic heads in the matrix, especially at the boundary between the matrix and the conduit.

Figure 4 presents the experimental and computational results of tracer evolution (visualised using a dye in the experiments) at several time instants. The results of the SD simulation are very similar to the experimental results,

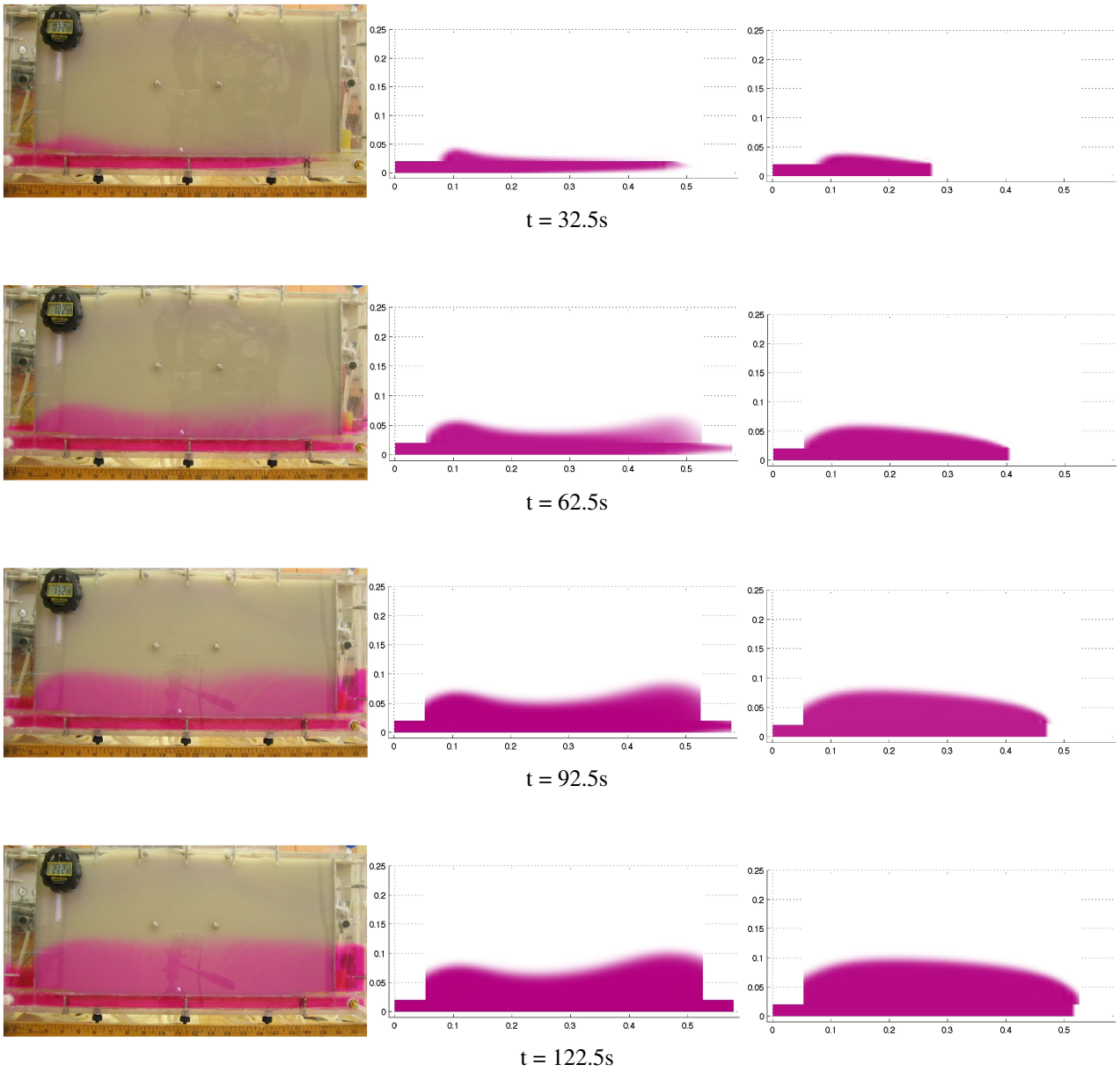

Figure 4. Experimental (left) and computational CCPF (middle) and SD (right) for solute concentration in the matrix at times $t = 32.5$ s, $t = 62.5$ s, $t = 92.5$ s and $t = 122.5$ s

but the CCPF simulation results are quite different. First, CCPF modelling underestimates the dye-front movement in the conduit as well as the dye exchange at the interface between the conduit and the matrix. Second, the modelling plume distribution in the matrix has a convex shape for the CCPF model and does not capture the characteristics of the plume distribution in the experiment, that is, a broad U-shape with two humps caused by the two end points of the interface. The SD simulations do capture these features of the experimental results. The results given in Figures 3 and 4 as well as other similar examples indicate that the SD model with the BJ interface condition is a valid model for coupled matrix–conduit flows and tracer transport. On the other hand, at least for the value of α_{ccpf} used in the calculations resulting in Figures 3 and 4, it seems that the CCPF model is not validated. The question remains: can other values of α_{ccpf} yield better results? This question is addressed next.

SENSITIVITIES OF MODELING PARAMETERS

Both the CCPF and the SD models contain a modelling parameter, α_{sd} and α_{ccpf}, respectively. In this section, we examined the sensitivity of solutions with respect to these parameters and also used experimental and computational results to gain some insight into the calibration of these parameters.

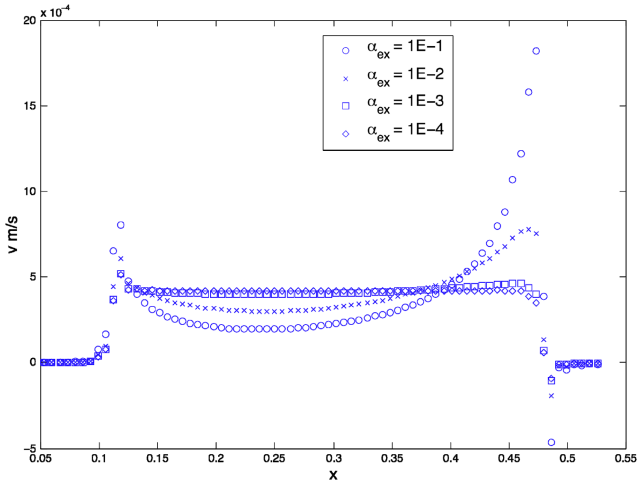

Figure 5. Normal velocity at the matrix–conduit interface for different values of the exchange rate coefficient α_{ccpf} in the CCPF model

As is pointed out and verified by (Bauer *et al*. (2003), Birk *et al*. (2003) and Liedl *et al*. (2003), the CCPF model is very sensitive to the value of exchange rate parameter α_{ccpf}. Those studies focussed on the small values of the parameter, that is, in the range of O(1) multiples of the hydraulic conductivity. It was noted that as α_{ccpf} varies over this range, which is approximately 0 to 10^{-3}, the breakthrough time of conduit genesis may vary over several orders of magnitude.

The high sensitivity of the CCPF model to variation in the exchange coefficient for small values of α_{ccpf} may also be gleaned from an examination of the equation from which that sensitivity may be determined. For simplicity, we considered the steady-state case. The formal differentiation of the steady-state version of Equations (10a) and (10b) with respect to α_{ccpf} yields the sensitivity equations

$$-\nabla\left(K\nabla h'_{m}\right)+\alpha_{ccpf}\left(h'_{m}-h'_{c}\right)\delta_{\Omega_c}=-\left(h_m-h_c\right)\delta_{\Omega_c}\ \text{in}\ \Omega_m \tag{12a}$$

$$-\frac{\partial}{\partial\tau}\left(D\frac{\partial h'_{c}}{\partial\tau}\right)-\alpha_{ccpf}\left(h'_{m}-h'_{c}\right)=\left(h_m-h_c\right)\ \text{along}\ \Omega_c \tag{12b}$$

for the sensitivities $h'_{m}=\partial h_m/\partial_\alpha$ and $h'_{mc}=\partial h_c/\partial\alpha$. Next, denote by $h_{m,0}{}'$ and $h_{c,0}{}'$ is the solution of Equations (10a) and (10b) for $\alpha_{ccpf}=0$; note that in this case, Equations (12a) and (12b) for the conduit pipe Ω_c and matrix Ω_m are uncoupled. Then, from Equations (12a) and (12b), we deduced that the sensitivities $h_{m,0}{}'$ and $h_{c,0}{}'$ evaluated at $\alpha_{ccpf}=0$ are determined from

$$-\nabla\left(K\nabla h'_{m,0}\right)=-\left(h_{m,0}-h_{c,0}\right)\delta_{\Omega_c}\ \text{in}\ \Omega_m \tag{13a}$$

$$-\frac{\partial}{\partial\tau}\left(D\frac{\partial h'_{c}}{\partial\tau}\right)=\left(h_{m,0}-h_{c,0}\right)\ \text{along}\ \Omega_c \tag{13b}$$

Now examine, for example, Equation (13a); $(h_m,0-h_{c,0})$ is of O(1), whereas K is of O(10^{-4}) so that $h_{m,0}{}'$ is of O(10^4).

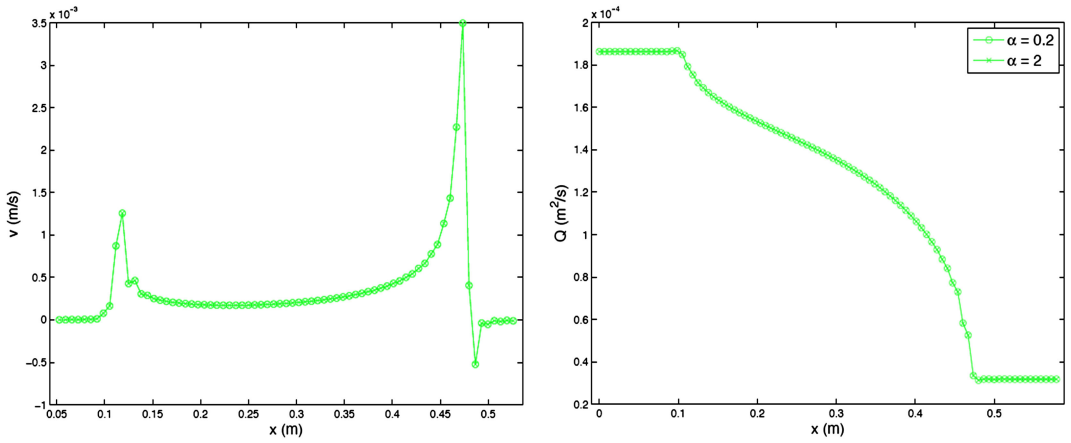

Figure 6. The exchange velocity (left) and conduit discharge (right) for the different values obtained from SD simulations with α_{sd}=0.2 and 2

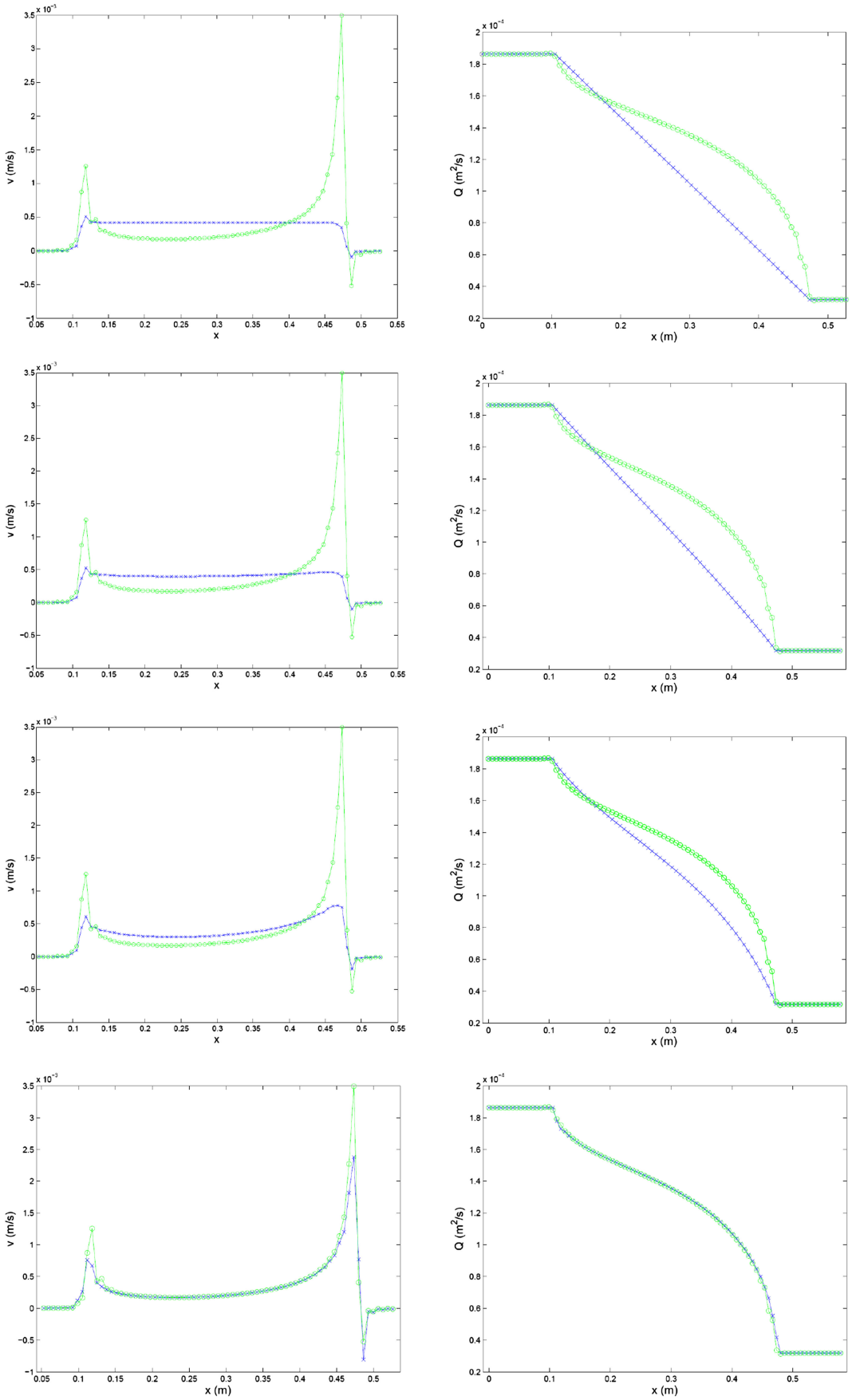

Figure 7. Comparison between SD (circles) and CCPF (hash marks) results for the exchange velocity (left) and conduit discharge (right) for the different values of the exchange rate coefficient α_{ccpf} in the CCPF model; top to bottom: $\alpha_{ccpf} = 10^{-4}$, 10^{-3}, 10^{-2} and 1

Thus, we see that h_m will change rapidly for small values of α_{ccpf}.

In general, quantities such as the exchange of fluid along the interface and the discharge in the conduit are sensitive to the choice of the value of the exchange parameter α_{ccpf}. In the laboratory experiment, the hydraulic conductivity of the glass beads is 6.19×10^{-4} m/s, so we set α_{ccpf} in the range of $[10^{-4}, 10^{-1}]$. Note that this is a range of larger values of α_{ccpf} than that used in the sensitivity studies by Bauer *et al.* (2003), Birk *et al.* (2003) and Liedl *et al.* (2003). As shown in Figure 5, the exchange flow rate at the matrix–conduit interface is very sensitive to the choice of α_{ccpf}. Note that for this study, we used discharge boundary condition at the inlet and outlet of the conduit pipe.

The SD model with the BJ interface condition seems to be much less sensitive with respect to its modelling parameter α_{sd}. In Beavers and Joseph (1967), it is suggested that α_{sd} should be chosen somewhere in the range [0.2, 2]. In Figure 6, we see that the exchange velocity and the conduit discharge for $\alpha_{sd} = 0.2$ and 2 are very nearly identical when the fixed inflow rate and outflow rate boundary conditions are specified for the conduit. Thus, we see that the results of this model are not very sensitive to changes in α_{sd}.

In the section on Experimental Validation of Simulation Models, we concluded that the SD model with the BJ interface condition produced results that were in good agreement with experimental results but that the CCPF model results were in not such good agreement for the parameter value $\alpha_{ccpf} = 7.4 \times 10^{-4}$. We also just concluded that the SD model is largely insensitive to the value of α_{sd}. Thus, we would like to determine if other values of α_{ccpf} might yield better results.

When using the CCPF model, we compared results using that model with different values of α_{ccpf} to those obtained by using the SD model with $\alpha_{sd} = 0.2$. In Figure 7, such comparisons are provided for four values of α_{ccpf}. We see that agreement improves as the value of α_{ccpf} increases and that for the largest value, the agreement between the CCPF and SD results are quite good. These results suggest the possibility that CCPF simulations of karst-like problems can be improved by using values for the exchange rate parameter α_{ccpf} that are larger than those that have been used in practice. Of course, a much more intensive study of this issue is needed before such a conclusion can be made definite. As mentioned earlier, this is a subject of our current work, which involves applying optimisation strategies to determine an optimal value for α_{ccpf} and for studying the dependence of the optimal value on other parameters defining the CCPF model.

SUMMARY AND CONCLUSIONS

In our previous study, Faulkner *et al.* (2009) developed the SD model for groundwater flow in a conduit–matrix system. Stokes equation was used to describe the flow in conduit, and the Darcy law is applied for flow in matrix, and the BJ interface condition is adopted to describe the interface between the conduit and the matrix. Cao *et al.* (2011) studied the mathematical well-posedness of the CCPF model as well as convergence rates of its finite element approximation. In this study, we used the analyses to validate a finite element SD simulation model. By using computational experiments, we also verified the implementation codes for the simulation model.

To compare with the currently used model, we reviewed the CCPF model for flows in conduit–matrix systems and the results of mathematical analyses of the model. We validated a finite element CCPF simulation model using numerical analyses and, using computational experiments, we verified the implementation codes for the simulation model.

The laboratory experiment of Faulkner *et al.* (2009) is used to provide data for further validation studies of the computer simulation models. The studies suggest that the SD model with the BJ interface condition is a valid model for conduit–matrix systems. On the other hand, perhaps the CCPF model with the value of the exchange parameter chosen within the range suggested in the literature does not result in good agreement with experimental observations. In particular, the CCPF model overestimates the hydraulic heads along the interface between the matrix and the conduit, underestimates solute transport in the conduit and does not capture well the plume distribution in the matrix.

We examined the sensitivity of the CCPF model with respect to the exchange parameter, concluding that, as other authors have previously noted, the model is highly sensitive for small values of the exchange parameter. However, for larger values, the model becomes less sensitive and, more important, also produces results that are in better agreement with experimental observations. This suggests that the CCPF model may also produce accurate simulation results, if one chooses larger values of the exchange parameter than those suggested in the literature. We also found that the SD model with the BJ interface is relatively insensitive to the value of the exchange parameter appearing in that model.

ACKNOWLEDGEMENT

This work was supported by the CMG program of the National Science Foundation under grant numbers DMS-0620035 and DMS-0620091.

REFERENCES

Barenblatt G, Zheltov I, Kochina I. 1960. Basic concepts in the theory of seepage of homogeneous liquids in fissured rocks. *Journal of Mechanics and Applied Mathematics (USSR)* **24**: 1286–1303.

Bauer S, Liedl R, Sauter M. 2000. Modeling of karst development considering conduit-matrix exchange flow. Calibration and reliability in groundwater modelling: coping with uncertainty. *IAHS Publication* **265**: 10–15.

Bauer S, Liedl R, Sauter M. 2003. Modeling of karst aquifer genesis: Influence of exchange flow. *Water Resources Research* **39**: 1285. DOI: 10.1029/2003WR002218

Bear J, Verruijt A. 1987. *Modeling Groundwater Flow and Pollution*. D. Reidl: Norwell, Mass.

Beavers G, Joseph D. 1967. Boundary conditions at a naturally permeable wall. *Journal of Fluid Mechanics* **30**: 197–207.

Birk S, Liedl R, Sauter M, Teutsch G. 2003. Hydraulic boundary conditions as a controlling factor in karst genesis. *Water Resources Research* **39**: 1004. DOI: 10.1029/2002WR001308

Bobok E. 1993. *Fluid Mechanics for Petroleum Engineers*. Elsevier: New York.

Cao Y, Gunzburger M, Hua F, Wang X. 2011. Analysis and finite element approximation of a coupled, continuum pipe-flow/Darcy model for flow in porous media with embedded conduits. *Numerical Methods for Partial Differential Equations* **27**(5): 1242–1252. DOI: 10.1002/num.20579

Cao Y, Wang H, Xie X. 1988. Dual-media flow models of karst areas and their application in north China. In *Karst Hydrogeology and Karst Environment Protection: 21st Congress of the International Association of Hydrogeologists*. Int. Assoc. of Hydrogeologists: Guilin, China.

Chen Y, Bian J. 1988. The media and movement of karst water. In *Karst Hydrogeology and Karst Environment Protection: 21st Congress of the International Association of Hydrogeologists*. Int. Assoc. of Hydrogeologists: Guilin, China.

Discacciati M, Miglio E, Quarteroni A. 2002. Mathematical and numerical models for coupling surface and groundwater flows. *Application of Numerical Mathematics* **43**: 57–74.

Faulkner J, Hu BX, Kish S, Hua F. 2009. Laboratory analog and Numerical study of groundwater flow and solute transport in a karst aquifer with conduit and matrix domains. *Journal of Contamination Hydrology* **110**: 34–44.

Ford D. 1998. Perspectives in karst hydrology and cavern genesis. *Bull Hydrogeol* **16**: 9–29.

Ford D, Williams P. 1989. *Karst Geomorphology and Hydrology*. Chapman and Hall: New York.

Gerke H, van Genuchten M. 1993a. A dual-porosity model for simulating the preferential movement of water and solutes in structured porous media. *Water Resources Research* **29**: 305–319.

Gerke H, van Genuchten M. 1993b. Evaluation of a first-order water transfer term for variably saturated dual-porosity models. *Water Resources Research* **29**: 1225–1238.

Hua F. 2009. Modeling, analysis and simulation of SD system with Beavers–Joseph interface condition. Ph.D. Thesis; Florida State University, Tallahassee.

Katz B, Catches J, Bullen T, Michel R. 1998. Changes in the isotopic and chemical composition of ground water resulting from a recharge pulse from a sinking stream. *Journal of Hydrology* **211**: 178–207.

Kincaid T. 2004. Exploring the secrets of Wakulla Springs, open seminar, Tallahassee.

Kiraly L. 1998. Modeling karst aquifers by the combined discrete channel and continuum approach. *Bull Hydrogeol* **16**: 77–98.

Kuniansky E. 2008. U.S. Geological Survey Karst Interest Group Proceedings. U.S. Geological Survey Scientific Investigations Report 2008–5023, Bowling Green.

Li G, Loper D, Kung R. 2008. Contaminant sequestration in karstic aquifers: experiments and quantification. *Water Resources Research* **44**: W02429. DOI: 10.1029/2006WR005797

Liedl R, Sauter M, Huckinghaus D, Clemens T, Teutsch G. 2003. Simulation of the development of karst aquifers using a coupled continuum pipe flow model. *Water Resources Research* **39**: 1057. DOI: 10.1029/2001WR001206

MacQuarrie K, Sudicky E. 1996. On the incorporation of drains into three dimensional variably saturated groundwater flow models. *Water Resources Research* **32**: 447–482.

Matusick J, Zanbergen P. 2007. Comparative study of groundwater vulnerability in a karst aquifer in central Florida. *Geophysical Research Abstracts* **9**: 04614.

Saffman P. 1971. On the boundary condition at the interface of a porous medium. *Studies in Applied Mathematics* **1**: 77–84.

Sauter M. 1992. Quantication and forecasting of regional groundwater flow and transport in a karst aquifer (*Gal lusquel le, Malm SW Germany*). Ph.D. Thesis; Univ. of Tubingen, Tubinger, Germany.

Shoemaker W, Kuniansky E, Birk S, Bauer S, Swain E. 2008. Documentation of a conduit flow process (CFP) for MODFLOW-2005. U.S. Geological Survey Techniques and Methods 6-A24.

Taylor C, Greene E. 2001. Quantitative Approaches in Characterizing Karst Aquifers: U.S. Geological Survey Karst Interest Group Proceedings. Water Resources Investigations Report 01–4011; 164–166.

Teutsch G. 1989. Two practical examples from the Swabian Alb, S. Germany. In Proc. 4th Conference on Solving Groundwater Problems with Models, Indianapolis.

Worthington S. 2003. A comprehensive strategy for understanding flow in a carbonate aquifer. *Speleogenesis and Evolution of Karst Aquifers* **1**: 1–8.